

Fermi-momentum dependence of relativistic effective mass below saturation from superscaling of quasielastic electron scattering

V.L. Martinez-Consentino,^{1,*} I. Ruiz Simo,^{1,†} J.E. Amaro,^{1,‡} and E. Ruiz Arriola^{1,§}

¹*Departamento de Física Atómica, Molecular y Nuclear
and Instituto Carlos I de Física Teórica y Computacional
Universidad de Granada, E-18071 Granada, Spain.*

(Dated: July 31, 2021)

The relativistic effective mass M^* , and Fermi momentum, k_F , are important ingredients in the determination of the nuclear equation of state, but they have rarely been extracted from experimental data below saturation density where translationally invariant nuclear matter becomes unstable against clusterization into the existing atomic nuclei. Using a novel kind of superscaling analysis of the quasielastic cross section electron scattering data involving a suitable selection criterion and ^{12}C as a reference nucleus, the global scaling properties of the resulting set of data for 21 nuclei ranging from ^2H to ^{238}U are then analyzed. We find that a subset of a third of the about 20000 data approximately scales to an universal superscaling function with a more constrained uncertainty band than just the reference ^{12}C case and provides M^* as a function of k_F .

PACS numbers: 24.10.Jv,25.30.Fj,25.30.Pt,21.30.Fe

Keywords: quasielastic electron scattering, relativistic mean field, relativistic Fermi gas, effective mass.

Since the early days of nuclear physics, the concept of nuclear matter has provided phenomenological guidance and has stimulated over the years benchmarking microscopic theoretical solutions of the many-body nuclear problem under the assumption of translational invariance. Below the saturation density $n_0 = 0.16 \text{ fm}^{-3}$, however, nuclear matter becomes unstable against cluster formation into the finite atomic nuclei; the equation of state of nuclear matter has no obvious meaning hindering an extraction of nuclear matter parameters such as the Fermi momentum or the effective mass from data. In the present work we undertake such a determination by a scaling analysis of a large body of inelastic electron-nucleus scattering data around the quasielastic (QE) peak.

Scaling is a powerful tool for analyzing the response of a complex system to weakly interacting probes from a variety of complex systems (see [1–4] and references therein). The probes include electrons, neutrons and neutrinos of different energies and the targets range from solids and liquids, to atoms, nuclei and nucleons. In the case considered here of inclusive electron scattering from nuclei, scaling has been exploited to analyze a large amount of QE data for different nuclei in terms of a phenomenological scaling function extracted from the cross section. It is a remarkable fact that the reduced cross section of different nuclei scale to the same function $f(\psi')$ of the scaling variable $\psi' = \psi'(q, \omega)$, for $\psi' < 0$ [2]. This indicates an universal behavior of the dynamics inside the

system that has been exploited with success for instance to predict neutrino cross sections from (e, e') data [5, 6]. The study of the longitudinal and transverse response functions allowed to extract a longitudinal scaling function $f_L(\psi')$ also for $\psi' > 0$ [7], unlike the transverse response, which does not scale. To obtain a proper value of the transverse scaling function $f_T(\psi') \neq f_L(\psi')$ one has to resort to the Relativistic Mean Field (RMF) model, which reproduces well the $f_L(\psi')$. In the SuSA-v2 model this transverse scaling function was updated in a fit to (e, e') data, requiring an additional q -dependence, with an explicit scaling violation [8], although this is not in full contradiction with the data.

In recent works [9, 10] we have performed a new kind of scaling analysis of the ^{12}C QE data [11]. The so-called super scaling analysis with relativistic effective mass $M^* = m_N^*/m_N$ (SuSAM*) is based on the Fermi gas in RMF as a starting point, modified by introducing a suitable scaling function $f^*(\psi^*)$. The scaling variable ψ^* depends, for each nucleus, on the Fermi momentum k_F and the relativistic effective mass m_N^* . This analysis benefits from several advantages related to the traditional y -scaling or the ψ -scaling [2–4, 12] for the study of the QE peak. First gauge invariance is preserved by using the effective mass instead of a separation energy as parameter to describe the center of the QE peak. Second, it exploits the good properties of RMF when describing the general features of the QE peak [13–15], by including the dynamics of the RMF into the definition of the scaling variable through the effective mass. As a consequence, the transverse response shows naturally the enhancement produced by the lower components of the nucleon spinors induced by the mean field. Third our approach allows to extract an unique scaling function $f^*(\psi^*)$ for $\psi^* > 0$ as well, directly from the cross section data.

In the present SuSAM* approach we write the QE cross

*Electronic address: victormc@ugr.es

†Electronic address: ruizsig@ugr.es

‡Electronic address: amaro@ugr.es

§Electronic address: earriola@ugr.es

section in factorized form

$$\left(\frac{d\sigma}{d\Omega d\omega}\right)_{\text{QE}} = \overline{\left(\frac{d\sigma}{d\Omega}\right)}_{en} \overline{N}_n(q, \omega) + \overline{\left(\frac{d\sigma}{d\Omega}\right)}_{ep} \overline{N}_p(q, \omega). \quad (1)$$

The electron-nucleon cross section averaged over the Fermi sea, $\overline{\left(\frac{d\sigma}{d\Omega}\right)}_{en,p}$, for nucleons with mass m_N^* , are obtained from the formalism of ref. [10]. These elementary cross sections are multiplied by the effective number of nucleons that can be excited by the electron per unit of energy transfer ω , and for given momentum transfer q . For neutrons it is given by

$$\overline{N}_n(q, \omega) = \frac{N\xi_F}{m_N^* \eta_F^3 \kappa} f^*(\psi^*) \quad (2)$$

and a similar definition for the effective number of protons \overline{N}_p . Here we use dimensionless variables $\kappa = q/(2m_N^*)$, $\eta_F = k_F/m_N^*$ and $\xi_F = (1 + \eta_F^2)^{1/2} - 1$. Note that the effective number of protons (neutrons) is not the true number in the relativistic case, because its integral over ω is less than the total number of protons (neutrons), and a kinematic correction normalization factor is needed to recover the sum rule.

The above expressions are exact in the RMF for infinite matter. The SuSAM* approach assumes that the scaling function $f^*(\psi^*)$ is an universal function valid for all nuclei. Here it is extracted from the QE (e, e') data of a large amount of nuclei. It depends on a single scaling variable defined as the minimum kinetic energy of the initial nucleon, divided by the Fermi kinetic energy. All the kinematics are referred to the RMF, where the nucleon mass is replaced by the relativistic effective mass m_N^* [10].

In Fig. 1 we show the scaled experimental data used in this work [11, 16]. The experimental scaling function data in Fig. 1 are computed from the experimental cross section data by inverting Eq. (1). They have been plotted against the scaling variable defined as

$$\psi^* = \sqrt{\frac{\epsilon_0 - 1}{\epsilon_F - 1}} \text{sgn}(\lambda - \tau) \quad (3)$$

where

$$\epsilon_0 = \text{Max} \left\{ \kappa \sqrt{1 + \frac{1}{\tau}} - \lambda, \epsilon_F - 2\lambda \right\}, \quad (4)$$

and we use the variables $\lambda = \omega/2m_N^*$, $\tau = \kappa^2 - \lambda^2$, and $\epsilon_F = \sqrt{1 + \eta_F^2}$. Note that in the traditional ψ -scaling variable is a particular case of these equations for $m_N^* = m_N$. In both cases the scaling variable is negative to the left of the QE peak ($\lambda < \tau$) and positive on the right side.

Note that the data in the top panel of Fig. 1 do not scale in general. Yet it is remarkable that a large fraction of the data collapse into a gray band that allows to define a “quasielastic” experimental region with a maximum for $\psi^* = 0$. The RFG scaling function is shown

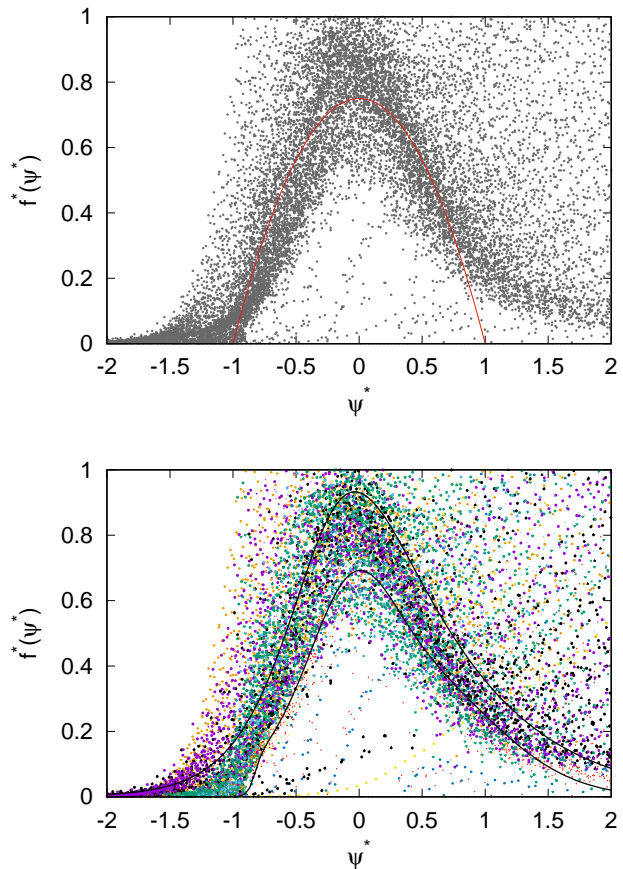


FIG. 1: Top panel: experimental scaling function $f^*(\psi^*)$ computed for all the nuclei in the database of ref. [4, 11, 16] compared to the RFG scaling function. Bottom panel the same data points are compared to the phenomenological band fitted to the selected subset of QE data (see text).

as the parabola in red to compare with. The data have been scaled with the values of Fermi momentum and effective mass given in columns 6 and 7 of Table I. These parameters have been obtained by a χ^2 fit to the scaling band shown in the bottom panel of Fig. 1. This band is parameterized as the sum of two Gaussians modified by a suitable Fermi function.

$$f^*(\psi^*) = \frac{a_3 e^{-(\psi^* - a_1)^2 / (2a_2^2)} + b_3 e^{-(\psi^* - b_1)^2 / (2b_2^2)}}{1 + e^{-\frac{\psi^* - c_1}{c_2}}} \quad (5)$$

The parameters of this scaling function are given in Table 2 as well as the lower, and upper limits of the boundary, defining the uncertainty band. The data lying outside the band correspond mainly to inelastic processes or to low energy excitations of the target nucleus, both processes breaking naturally scaling not being quasi-free. The rest of them inside the band correspond approximately to quasi-free events, the fluctuations generating the band could be produced by reactions mechanisms beyond the impulse approximation, including FSI, nuclear correlations, meson-exchange currents, multi-nucleon knockout,

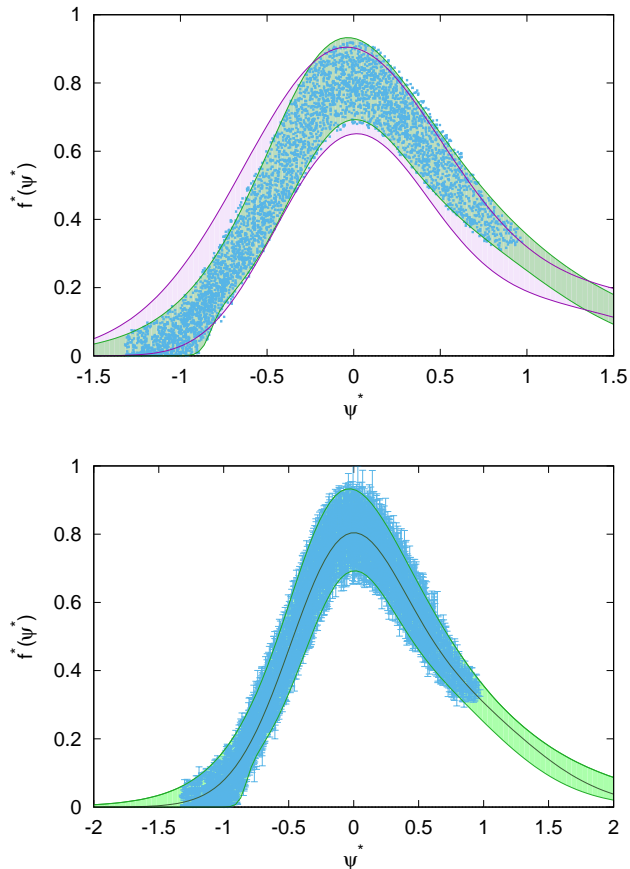


FIG. 2: Top panel: the starting band in pink of ^{12}C compared to the new fit and to the selected data from all the nuclei. Bottom panel: the fitted band compared to the selected data with errors. Data are from ref. [4, 11, 16]

or related processes.

To obtain the scaling band is a two-step procedure. We have started with the scaling function already fitted in ref. [10] for ^{12}C , with parameters $M^* = 0.8$ and $k_F = 225$ MeV/c. Our hypothesis is that this starting band, shown in the top panel of Fig. 2, is approximately valid for every nucleus. Thus, in this first step we visually tune the parameters M^* and k_F for each nucleus separately so that the maximum of the QE peak occurs approximately at $\psi^* = 0$ and its width agrees with the ^{12}C band. The resulting parameters are shown in the second and third columns of Tab. I.

With these parameters we have scaled all the data selected from those kinematics where the QE peak is clearly visible. We have therefore eliminated all the kinematics where only the inelastic or deep inelastic region are present corresponding to very large momentum and energy transfer. In the same way we have also discarded the very low energy kinematics where the peak occurs at $q < 100$ MeV/c and scaling is violated. We have only included the nuclei with more than 45 QE data points from Table I. With this set of data (not shown) a second

Nucleus	Visual fit		no. points fit		χ^2 fit		no. points	
	k_F	M^*	k_F	M^*	k_F	M^*	QE	Total
^2H	80	1.00	88	0.99	115	0.99	426	2135
^3H	120	0.97	142	0.99	136	0.98	139	540
^3He	140	0.95	147	0.96	136	0.99	794	2472
^4He	160	0.90	180	0.89	180	0.86	803	2718
^6Li	165	0.80	—	—	175	0.77	23	165
^9Be	185	0.80	—	—	202	0.85	16	390
^{12}C	225	0.80	226	0.82	217	0.80	660	2883
^{16}O	230	0.80	259	0.84	250	0.79	48	126
^{24}Mg	235	0.75	—	—	238	0.65	23	34
^{27}Al	236	0.80	258	0.78	249	0.80	75	628
^{40}Ca	240	0.73	250	0.73	236	0.71	616	1339
^{48}Ca	247	0.73	242	0.75	237	0.71	728	1227
^{56}Fe	238	0.70	240	0.79	241	0.70	485	2429
^{59}Ni	235	0.67	—	—	238	0.65	27	37
^{89}Y	235	0.65	—	—	224	0.64	27	37
^{119}Sn	235	0.65	—	—	232	0.64	24	34
^{181}Ta	235	0.65	—	—	232	0.64	24	33
^{186}W	230	0.77	—	—	226	0.76	45	184
^{197}Au	240	0.75	—	—	238	0.78	30	96
^{208}Pb	237	0.65	239	0.64	233	0.56	818	1714
^{238}U	259	0.65	219	0.59	219	0.51	193	420

TABLE I: Values of the parameters M^* and k_F (in MeV/c) obtained from the different fits to the scaling band.

selection has been done by applying the density criterion of Ref. [9, 10]. We have kept only the data surrounded by more than 160 points inside a circle of radius $r = 0.1$ in the plot.

In Fig. 2 we show the resulting set of selected data. With these data we have fitted the green band parameterized with Eq. (5), which is compared to the starting ^{12}C scaling band of ref. [10]. The new band turns out to be slightly different and thinner than the starting ^{12}C band. These differences arise because the selection procedure has been improved with respect to ref. [10]. We have verified that the nuclei with few QE points and not selected are basically inside the fitted band, hence they do not influence the determination of the band nor the results on Fig. 2. In the bottom panel of Fig. 2 we show again the surviving points with error bars compared to the fitted band.

Starting with the parameterized band, Eq. (5), two additional fits of M^* and k_F , have been performed. First we have maximized the number of points inside the band. The results are shown in columns 4 and 5 of Tab. 1. The values are compatible with those estimated before, specially in the cases where the number of QE data points is large. However an unambiguous determination of the effective mass and Fermi momentum has not been possible by this method for some nuclei, due to the small number of data (their values are not given in the columns 4 and 5 of Table I).

To estimate the uncertainty on the parameters, we have performed a third fitting procedure by minimizing the χ^2 function constructed from the sum of the squared

	a_1	a_2	a_3	b_1	b_2	b_3	c_1	c_2
central	-0.1335	0.4319	1.3885	0.5741	0.6539	0.6083	0.3405	2.2947
min	0.3075	-0.6898	0.4115	-0.0647	-0.3145	0.3267	-0.8362	0.0295
max	-7.0719	-2.4644	38.58	-7.0724	-2.4595	38.58	-0.2613	0.2410

TABLE II: Parameters of our fit of the phenomenological scaling function central value, $f^*(\psi^*)$, and of the lower and upper boundaries (min and max, respectively).

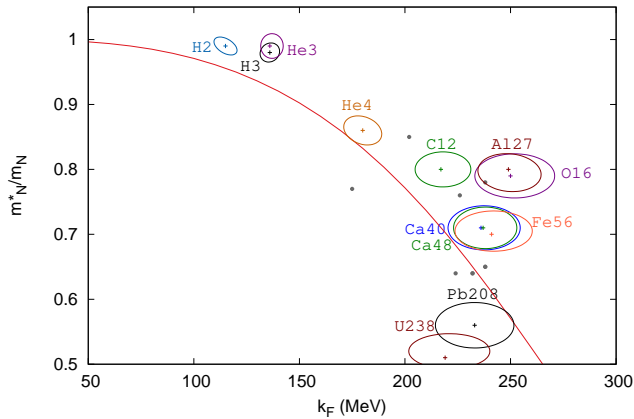


FIG. 3: Values of the effective mass represented against the Fermi momentum for all the nuclei considered in the χ^2 fit. The solid line corresponds to the $\sigma - \omega$ model of Ref. [14].

distances to the band center divided by the band width squared plus the experimental error added in quadrature. As a result we obtained the scaled data already shown in Fig. 1. Besides, this fit allows to compute the statistical errors of the parameters. Only the kinematics where the QE peak is clearly visible are included in the fit, and only those data where the momentum transfer is large enough (at least above $q = 100$ MeV/c) to avoid very low energy excitation contributions.

In figure 3 we show the χ^2 -fitted values of M^* against the Fermi momentum, and their 1σ confidence intervals, represented by ellipses. With this plot our scaling analysis of the QE peak for finite nuclei can be related to different realizations (different k_F values) of nuclear matter below saturation. For comparison we show the theoretical dependence $M^*(k_F)$ obtained within the RMF in the $\sigma - \omega$ model of Ref. [14] of nuclear matter. The points

show a similar trend although there is room for improvements. On the other hand our extracted data provide constraints for theoretical determinations of the nuclear equation of state.

In the above results the super-scaling hypothesis — that there is an universal function $f^*(\psi^*)$ for all nuclei— was verified within an uncertainty band extracted from the data. However, such an extraction can be done in multiple ways within the allowed uncertainty. Thus, in order to test the robustness of our results we proceed as follows: after the χ^2 fit to the parameterized band, we generate a second band which is similar to the previous one, and a new χ^2 fit returns similar values within the present uncertainties.

To conclude, we have developed a method to obtain the relativistic effective mass for different values of the Fermi momentum using the superscaling of the QE data. Our method allows to predict the M^* values for Fermi momentum below the nuclear matter saturation point $k_F \sim 270$ MeV/c, corresponding to finite nuclei, and providing constraints on a empirical determination of the nuclear equation of state. We have also shown that the (e, e') data allow to extract a phenomenological scaling function with an uncertainty band in the QE region. The scaling function is valid for all nuclei studied—within their uncertainties— and points to an universality in the dynamics of the QE peak. These results will allow to provide predictions for other nuclei and other reactions of interest, for example in neutrino scattering from nuclei, of interest for the neutrino oscillation experiments.

This work is supported by Spanish DGI (grant FIS2014-59386-P) and Junta de Andalucía (grant FQM225). V.L.M.C. acknowledges a contract with Universidad de Granada funded by Junta de Andalucía and Fondo Social Europeo. I.R.S. acknowledges support from the Ministerio de Economía y Competitividad (grant Juan de la Cierva-Incorporación).

[1] I. Sick, D. Day, and J.S. Mc Carthy, Phys. Rev. Lett. **45**, 871 (1980).
[2] T. W. Donnelly and I. Sick, Phys. Rev. Lett. **82**, 3212 (1999).
[3] T. W. Donnelly and I. Sick, Phys. Rev. C **60**, 065502 (1999).
[4] O. Benhar, D. Day, and I. Sick, Rev.Mod.Phys. **80**(2008)189.
[5] J. E. Amaro, M. B. Barbaro, J. A. Caballero, T. W. Don-

nelly, A. Molinari, I. Sick, Phys. Rev. C **71**,015501(2005).
[6] G.D. megias, J. E. Amaro, M. B. Barbaro, J. A. Caballero, T. W. Donnelly, Phys. Lett. B **725** (2013) 170.
[7] C. Maieron, T. W. Donnelly and I. Sick, Phys. Rev. C **65**, 025502 (2002).
[8] G. D. Megias, J. E. Amaro, M. B. Barbaro, J. A. Caballero and T. W. Donnelly, Phys. Rev. D **94**, 013012 (2016).
[9] J. E. Amaro, E. Ruiz Arriola and I. Ruiz Simo, Phys.

- Rev. C **92**, no. 5, 054607 (2015).
- [10] J. E. Amaro, E. Ruiz Arriola and I. Ruiz Simo, Phys. Rev. D **95**, 076009 (2017).
- [11] O. Benhar, D. Day, and I. Sick, <http://faculty.virginia.edu/qes-archive/>.
- [12] W.M. Alberico, A. Molinari, T.W. Donnelly, E. L. Kronenberg, and J.W. Van Orden, Phys Rev. C 38 (1988) 1801.
- [13] R. Rosenfelder, Ann. Phys. (N.Y.) 128, 188 (1980).
- [14] B.D. Serot, and J.D. Walecka, Adv.Nucl.Phys.16(1986)1.
- [15] K. Wehrberger, Phys. Rep. 225 (1993) 273.
- [16] O. Benhar, D. Day and I. Sick, arXiv:nucl-ex/0603032.